Hindawi
Journal of Sensors
Volume 2020, Article ID 8523170, 10 pages
https://doi.org/10.1155/2020/8523170

Research Article

Thermal Noise-Boosting Effects in Hot-Wire-Based Micro Sensors

Massimo Piotto,[1,2] **Alessandro Catania**,[1] **Andrea Nannini**,[1] **and Paolo Bruschi**[1,2]

[1]*Dipartimento di Ingegneria dell'Informazione, University of Pisa, 56122 Pisa, Italy*
[2]*IEIIT-PISA, CNR, 56122 Pisa, Italy*

Correspondence should be addressed to Paolo Bruschi; paolo.bruschi@unipi.it

Received 28 October 2019; Accepted 12 December 2019; Published 7 January 2020

Guest Editor: Graziella Scandurra

Copyright © 2020 Massimo Piotto et al. This is an open access article distributed under the Creative Commons Attribution License, which permits unrestricted use, distribution, and reproduction in any medium, provided the original work is properly cited.

This article proposes an original approach aimed at modelling the noise density in sensors based on a single hot wire or pairs of thermally coupled wires. The model consists in an original combination of a previous electrothermal model of the wire with well-established assumptions on the thermal noise in conductors that carry moderate current densities. A simple method for estimating the model parameters with simple impedance spectroscopy is suggested. The predicted power spectral densities of the wire thermal noise differ from the result of previously presented analytical models, stimulating further experimental studies. The effects of the electrothermal feedback of both hot wires and hot-wire pairs on flicker noise is also intrinsically covered by the proposed approach.

1. Introduction

Hot wires are used in a large variety of sensing devices and instruments. They consist of thin wires of an electrical conductor that, once biased with a sufficiently large current, reach a temperature that is significantly larger than ambient temperature. Hot wires are generally suspended at the extremities and immersed in a fluid. The category of hot-wire devices includes hot films, which consist of a thin or thick conducting stripe deposited over a thermally and electrically insulating substrate. The temperature difference between the wire and the fluid (overheating) is detected exploiting the dependence of the electrical resistance on temperature. Measuring the overheating, it is possible to detect several quantities of interest. Sensors based on hot wires gained significant importance since they can be easily fabricated using MEMS (Microelectromechanical Systems) technologies that allowed extreme miniaturization leading to reduction of the power consumption and response time of up to three orders of magnitude with respect to traditional macroscopic devices.

Among the sensors that exploit this principle are vacuum sensors [1–3], gas concentration sensors [4], thermal conductivity probes [5], and anemometers [6–8]. An evolution of the single hot wire is represented by the pair of thermally coupled wires. These devices are formed by two hot wires placed at micrometric distances from each other, so that substantial thermal exchange occurs between them. Such an arrangement allows detection of both the magnitude and direction of airflows [9]. Recently, wire pairs with thermal mass as small as to allow temperature variations with frequencies up to several kHz have been used to detect the local fluid displacement induced by an acoustic wave [10–13]. In particular, this new class of sensors is capable of directly detecting the acoustic particle velocity (APV), enabling interesting applications that cannot be easily achieved with standard microphones [14]. In all the mentioned applications of hot wires, it is of primary importance to model the electrical noise produced by the wire, in order to estimate the actual resolution of the sensors. This aspect is very critical for the APV sensors, which are marked by relatively low sensitivities resulting in low signal-to-noise ratios even in the presence of large sound intensities.

Noise in electrical conductors supplied with a dc current is due to two main phenomena, namely, thermal agitation of the charge carriers (Johnson-Nyquist noise or thermal noise) and resistance fluctuations, resulting in the well-known flicker noise. Thermal noise is universal and is related only to the wire resistance and temperature, while flicker noise is strongly material-dependent. Both types of noise cause

fluctuations of the current and voltage of the wire, resulting in small fluctuations of the heating power.

In hot wires, these power fluctuations have to be taken into account because they generate nonnegligible temperature fluctuations, due to the high thermal isolation of the conductor. The high TCR (temperature coefficient of resistance) of the wire material transforms the temperature fluctuations again into voltage and current variations, in a loop. The effect of this thermoelectrical feedback on the noise density has not been studied extensively so far, maybe because the thermal capacity of macroscopic hot wires allows development of temperature fluctuations only in the range of ultralow frequencies (typically sub-1 Hz). This is no more the case for MEMS sensors, where cut-off frequencies in the kHz range are common. This electrothermal feedback was described previously by Kohl et al. [15], highlighting its consequences on the sensitivity and noise of metal film resistance bolometers. The same phenomenon was observed earlier in bolometers based on superconductor materials [16].

It should be recalled that the temperature of a body is subjected to temperature fluctuation even when the cited electrothermal cause is not present. This type of "natural" temperature fluctuations is due to the so-called phonon noise and has a total mean square value equal to $<\delta T^2> = k_B T^2/C_{\mathrm{TH}}$, where T is the body temperature, k_B the Boltzmann constant, and C_{TH} the thermal capacity of the body. Obviously, even these temperature fluctuations produce resistance fluctuations, resulting in voltage noise when the wire is biased with an electrical current. Furthermore, resistance fluctuations modulate the heating power, so that, in thermally insulated wires, the electrothermal feedback affects also phonon noise. This work is focused on the changes produced by the electrothermal feedback on thermal noise and flicker noise, with particular emphasis on the former. Therefore, analysis of phonon noise is out of the scope of this paper, although its contribution can be dominant in the case of materials with particularly high TCRs [17].

In Kohl et al.'s work [15], a model that implicitly takes into account the effects of the feedback on thermal noise was proposed. The limit of the approach proposed in [15] is, in our opinion, the use of an expression for the thermal noise voltage density that is valid only for electrical networks in perfect thermal equilibrium.

In this paper, we present an alternative noise model that starts from well-established assumptions on the very basic phenomena that generate current fluctuations in conductors and then applies the electrothermal feedback in a direct and rigorous way. Different noise expressions are found for both single hot wires and pairs of thermally coupled wires. Depending on the sign of the TCR and the type of biasing used for the wire (e.g., constant voltage or constant current), the model predicts significant modifications of the noise spectra with respect to the case of standard conductors, where the low thermal insulation prevents the development of significant self-heating, disrupting the quoted feedback mechanism. The main differences with respect to the previously proposed approach [15] are highlighted. This manuscript does not include experimental results but, on the other hand, intends to be a stimulus for the execution of measurements that, if interpreted on the basis of the model prediction, could add useful information for the design of hot-wire sensors.

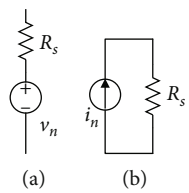

Figure 1: Thevenin (a) and Norton (b) representations of the noise in a resistor.

2. Electrothermal Model for Suspended Microwires

2.1. Noise in Wires out of Thermal Equilibrium. In thermal equilibrium, an electrical conductor will produce only thermal noise. In a Thevenin equivalent, a noiseless resistor is placed in series to a voltage noise source of PSD (Power Spectral Density) equal to $4k_B T R_S$, where k_B is the Boltzmann constant, T the absolute temperature, and R_S the conductor resistance. The Norton equivalent circuit consists of a noiseless resistor in parallel with a noise current source of PSD equal to $4k_B T G_S$, where $G = 1/R_S$. The two circuits are recalled in Figures 1(a) and 1(b). The first theoretical derivation of these noise models, developed by H. Nyquist using thermodynamic arguments, dates back to 1928.

Use of the above model to represent the noise in hot wires is not rigorous for two reasons. First, the voltage vs. current dependence (V-I curve) is not linear, due to self-heating and the relatively large TCR, so that defining the wire resistance is not straightforward. Second, a hot wire in operating conditions carries a nonzero electrical current and then is not in thermal equilibrium.

Let us start from the nonlinearity problem and consider Figure 2(a), where the V-I characteristics of a wire subjected to self-heating is sketched for the case of positive TCR.

For any given operating point, marked by current I and voltage V, we can define two resistances, namely, a large signal resistance, R, and a small-signal resistance, r_{DC}:

$$R = V/I, \tag{1}$$

$$r_{\mathrm{DC}} = \left.\frac{dV}{dI}\right|_{I,V}. \tag{2}$$

As the current increases, so does the overheating and, due to the assumption of positive TCR, also R increases, producing the nonlinear behaviour of the V-I characteristic shown in Figure 2(a). On the other hand, r_{DC} is the small-signal equivalent resistance. This resistance is applicable for variations around the operating point that are either constant (dc components) or slow (low frequencies) so as to allow the overheating to follow the heating power. At high frequencies, the thermal mass of the wire dampens the temperature variations and the equivalent small-signal resistance asymptotically tends to R. In between, the magnitude of the small-

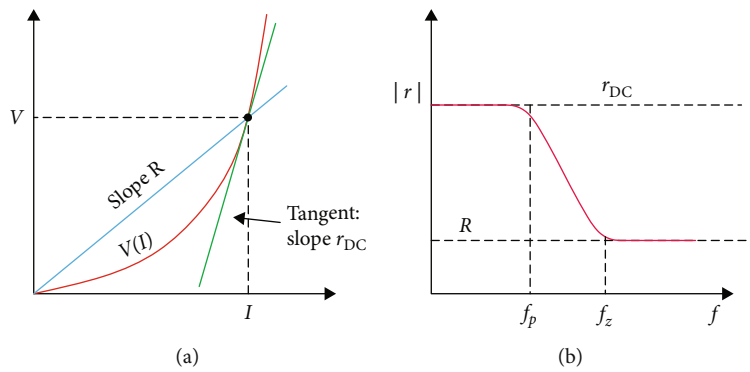

Figure 2: Sketched characteristics of a thermally insulated wire with positive TCR: (a) V-I plots; (b) magnitude of the small-signal impedance as a function of frequency.

signal (complex) impedance, indicated with r, should reasonably follow a bode plot like that depicted in Figure 2(b). The exact expression of the small-signal impedance, which is in agreement with this intuitive behaviour, was derived in a previous study [15], which deals with thermistor-based bolometers.

Since noise consists in small current and voltage variations around the operating point, the equivalent circuits of Figure 1 are applicable to the wire once R_s is replaced with the small-signal impedance r. What is less obvious is the expression of the spectral density to be assigned to v_n or i_n noise sources that appear in Figures 1(a) and 1(b), respectively, due to the mentioned nonequilibrium condition. It has been shown with either a semiclassical [18] or quantum mechanics [19] approach that the current fluctuation due to thermal agitation of the carriers has a spectral density that does not change when the conductor is subjected to a moderate dc current with respect to the case of thermal equilibrium. The reason is that the carrier drift velocity is much smaller than the thermal velocity in most practical cases of metallic conductors, so that the random walks of the carriers, from which the current fluctuation originates, are practically unaltered. These random walks depend on the same scattering mechanism from which the resistance R originates. Therefore, it is reasonable to consider that the current fluctuation has a spectral density equal to $4k_BT/R$. However, using this spectral density for the current source in the equivalent model of Figure 1(b) means neglecting the mentioned feedback effect that occurs in the hot wire. If the wire is biased with a constant voltage, a current change due to the random agitation of the carriers produces a variation of the heating power and, in turn, a change of the wire temperature and resistance R. The resulting resistance variation produces an additional current contribution that reinforces or diminishes the original current change depending on the sign of the TCR. Then, due to the wire self-heating, the actual current fluctuations seen from the wire terminals are different from those that would be predicted assigning the density $4k_BT/R$ to the current source in the circuit of Figure 1(b).

This electrothermal feedback effect was described in previous works on bolometers [15, 16], where the interest was mainly to model the effects on the device sensitivity. The feedback was also considered for its effect on thermal noise, and the authors simply propose to calculate the voltage noise power density as $4k_BT\,\mathrm{Re}\,(r)$, where "Re (r)" indicates the real part of impedance r. This approach was demonstrated to be applicable to RLC (resistance, inductance, and capacitance) networks in thermal equilibrium, but there is no physical justification for use of it for out-of-equilibrium systems in the presence of electrothermal feedback.

The alternative approach proposed in this work starts from the following equation for the total current (I) through a conductor subjected to a voltage V, valid also in the presence of self-heating:

$$I = \frac{V}{R} - i_e \Longleftrightarrow V = IR + Ri_e, \tag{3}$$

where i_e is the thermal noise component, marked by the usual spectral density $S_{\mathrm{IT}} = 4k_BT/R$, and R is simply defined by the ratio V/I_{drift}, where I_{drift} is the current component due only to the electric field in the conductor. Notice that the temperature dependence of R is the cause of the electrothermal feedback. To complete the framework, we consider also that R is subjected also to random fluctuations that would be present also in the case of a perfectly constant temperature. These fluctuations, indicated with δR_e, are the cause of flicker noise and can be boosted by the feedback as thermal noise. These are the premises that will be used in the next subsections to derive a model of the noise in single hot wires and in thermally coupled pairs of hot wires. All the models used in this work are of the lumped-element type. Therefore, quantities such as the wire temperature will represent averages calculated along the wire length.

2.2. Electrothermal Model of a Single Hot Wire. Figure 3 schematically shows the elements of the single wire model.

In the electrical domain, the wire is represented by voltage V across its terminals and current I flowing through it. The two quantities are tied by the electrical resistance R, as shown by Equations (1) and (2). In the thermal domain, the wire is characterized by its absolute temperature T, by its thermal capacity C_{TH}, and by thermal conductivity θ from the wire to the environment, which is considered to be at

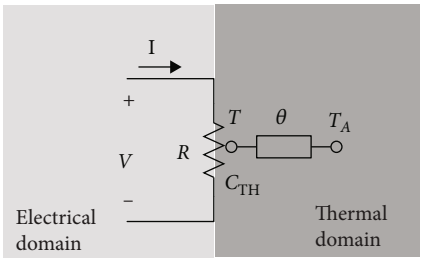

Figure 3: Elements of the electrothermal model for a single wire.

uniform temperature T_A. Thermal conductivity θ includes (i) heat conduction along the solid suspension elements, (ii) conduction and convection through the surrounding fluid, and (iii) radiation. We will consider that both R and θ are temperature-dependent quantities, while C_{TH} will be considered constant. Heat balance in the wire body will require that

$$C_{\mathrm{TH}}\frac{dT}{dt} = W - \theta(T - T_A), \tag{4}$$

where W is the total heating power dissipated by the electrical current, simply given by

$$W = V \cdot I. \tag{5}$$

In order to calculate the effects of fluctuations i_e and δR_e, it is convenient to use a small-signal analysis of the wire around a static operating point (dc components). Then, we can write

$$\begin{aligned} V &= V_0 + v, \\ I &= I_0 + i, \\ T &= T_0 + \delta T, \\ W &= W_0 + w, \end{aligned} \tag{6}$$

where V_0, I_0, T_0, and $W_0 = V_0 I_0$ define the operating point (OP) and v, i, δT, and w are the corresponding variations around the OP. We use lower-case symbols for v, i, and w since it is customary in small-circuit analysis of electrical circuits. For all other variations, we have used the prefix "δ." Taking into account the temperature dependence of R and θ, their first-order approximations can be written as

$$\begin{aligned} R &= R_0 + \alpha R_0 \delta T + \delta R_e, \\ \theta &= \theta_0 + \beta\theta_0 \delta T \text{ with } \alpha = \frac{1}{R}\frac{dR}{dT}, \\ \beta &= \frac{1}{\theta}\frac{d\theta}{dT}, \end{aligned} \tag{7}$$

where we have included also possible temperature independent fluctuations (δR_e) of R. Note that α is the TCR of the wire. Thermal equilibrium in the OP requires

$$W_0 = I_0 V_0 = \theta_0 (T_0 - T_A). \tag{8}$$

With the above definitions, the following equation for variations in the Laplace domain can be derived from Equation (4):

$$sC_{\mathrm{TH}}\delta T = w - \beta\theta_0 (T - T_A)\delta T - \theta_0 \delta T, \tag{9}$$

from which we find

$$\delta T = \gamma(s) w, \tag{10}$$

$$\gamma(s) = \frac{\gamma_0}{1 + s/\omega_g}, \tag{11}$$

$$\gamma_0 = \frac{1}{\theta_0[1 + \beta(T - T_A)]}, \tag{12}$$

$$\omega_g = \frac{1}{C_{TH}\gamma_0}. \tag{13}$$

In terms of variations, Equations (3) and (5) become

$$v = iR_0 + (\alpha R_0 \delta T + \delta R_e) I_0 + R_0 i_e, \tag{14}$$

$$w = iV_0 + vI_0. \tag{15}$$

Combining Equations (10)–(15), we can find with elementary algebraic passages

$$v = iR_0 \frac{1 + \alpha V_0 I_0 \gamma(s)}{1 - \alpha R_0 I_0^2 \gamma(s)} + \frac{R_0}{1 - \alpha R_0 I_0^2 \gamma(s)} i_e + \frac{I_0}{1 - \alpha R_0 I_0^2 \gamma(s)} \delta R_e, \tag{16}$$

which can be synthetically written in the following way:

$$v = i \cdot r + i_e \cdot r_e + k_R \delta R_e, \tag{17}$$

where coefficients r, r_e, and k_R depend on the complex frequency s. This dependence can be made more explicit, by substituting the expression of $\gamma(s)$ from Equation (11) into Equation (16) obtaining

$$r = R_0 \frac{1 + \alpha V_0 I_0 \gamma_0}{1 - \alpha V_0 I_0 \gamma_0} \cdot \frac{1 + s/\omega_z}{1 + s/\omega_p}, \tag{18}$$

$$r_e = R_0 \frac{1}{1 - \alpha V_0 I_0 \gamma_0} \cdot \frac{1 + s/\omega_g}{1 + s/\omega_p}, \tag{19}$$

$$k_R = \frac{I_0}{1 - \alpha V_0 I_0 \gamma_0} \cdot \frac{1 + s/\omega_g}{1 + s/\omega_p}, \tag{20}$$

where the following angular frequencies have been introduced:

$$\omega_z = \omega_G (1 + \alpha W_0 \gamma_0), \tag{21}$$

$$\omega_p = \omega_G (1 - \alpha W_0 \gamma_0). \tag{22}$$

Equations (17)–(22) can be used to describe the small-signal behaviour of the wire. As far as the small-signal ac impedance of the wire is concerned, this is given by

parameter r. It can be easily shown that for a positive TCR, the magnitude of r depends on the frequency as in Figure 2(b), with $f_p = \omega_p/2\pi$ and $f_z = \omega_z/2\pi$. An equivalent expression was found in [15].

Equation (17) can be used to find Thevenin and Norton representations of the wire noise. Referring to Figures 1(a) and 1(b), obviously, we have to replace resistor R_S with the complex impedance r in both the Thevenin and Norton circuits, in order to correctly model the ac behaviour of the wire. In the case of the Thevenin equivalent circuit, the voltage of the equivalent source (V_n in Figure 1(a)) can be calculated by nulling the small-signal current through the wire terminals (i.e., we set $i = 0$ in Equation (17)). This represents the case of a wire biased with a constant current (zero variations). Then, the PSD of the Thevenin equivalent noise source is given by

$$S_{vn} = 4k_B \frac{T_0}{R_0} |r_e|^2 + S_{\delta R_e}(f)|k_R|^2, \tag{23}$$

where $S_{\delta R_e}$ is the PSD of resistance fluctuations δR_e, while the PSD of i_e was assumed to be equal to $4k_B T_0/R_0$ as anticipated in the previous subsection. At high frequency, r_e tends to R_0, so that the thermal noise voltage contribution is simply $4k_B T_0 R_0$. Since also the complex impedance of the wire tends to R_0, the high-frequency limit simply corresponds to calculating the noise PSD using the usual Johnson-Nyquist expression. At very low frequencies ($f \ll f_p$), the thermal component of the voltage PSD becomes

$$S_{vn-th} = 4k_B T_0 R_0 \left| \frac{1}{1 - \alpha V_0 I_0 \gamma_0} \right|^2. \tag{24}$$

For a positive TCR ($\alpha > 0$), the denominator can approach zero when the static heating power $W_0 = V_0 I_0$ is large enough. In that case, the voltage noise PSD can get much larger than the high-frequency limit. It can be easily verified that the low-frequency limit given by Equation (24) does not coincide with the value obtained by applying the Jonson-Nyquist expression with the low-frequency limit of the wire resistance (r_{DC}) given by Equation (18) for $s = 0$.

A similar boosting effect can be observed for the flicker component, represented by the resistance fluctuation component. At high frequency, k_R tends to I_0, so that the voltage noise is simply given by the product of the resistance fluctuations and the bias current I_0. At low frequency, this term is boosted by the same factor as the thermal noise.

The noise voltage density of the Thevenin model represents the actual noise that should be expected when the wire is biased at constant current. It is interesting to observe that the boosting factor tends to infinity when $\alpha V_0 I_0 \gamma_0$ tends to one. If $\alpha V_0 I_0 \gamma_0$ gets larger than one, the pole $s_p = -\omega_p$ in the denominator of both r_e and k_R becomes positive, denoting instability. In these conditions, a small variation due to noise triggers a catastrophic increase of the voltage, leading to failure. This phenomenon is the well-known thermal runaway. It is possible to find a notable expression for $\alpha V_0 I_0 \gamma_0$ when thermal conductance θ is assumed to be independent of temperature ($\beta = 0$). In that case, $\gamma_0 = 1/\theta_0$ and $\alpha V_0 I_0 \gamma_0 = \alpha(T_0 - T_A)$. As a result, the noise-boosting factor $(1 - \alpha V_0 I_0 \gamma_0)^{-1}$ tends to infinity when the product of the wire overheating $(T_0 - T_A)$ by the TCR tends to one. Thermal runaway occurs when this product is equal to or greater than one. For a negative TCR, Equation (24) predicts a noise reduction at low frequencies with respect to the $4k_B T_0 R_0$ limit and no thermal runaway.

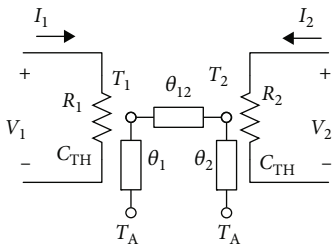

Figure 4: Elements of the electrothermal model for a thermally coupled wire pair.

The situation is reversed for the Norton equivalent model. The noise current source of the Norton model gives the current fluctuations when the wire is biased at constant voltage. Its value can be found setting $v = 0$ in Equation (17) and solving for current variations i, finding

$$i_n = -i = \frac{r_e}{r} i_e + \frac{k_R}{r} \delta R_e. \tag{25}$$

Ratios r_e/r and k_R/r are now marked by a pole equal to $-\omega_z$. Instability, i.e., thermal runaway, occurs when the TCR is negative. This is a well-known difference between constant-current and constant-voltage biasing. Similarly, current noise boosting at low frequency occurs only for $\alpha < 0$. In particular, the thermal component of the noise current PSD in the low-frequency limit that can be found from Equation (25) is

$$S_{in-th} = 4k_B \frac{T_0}{R_0} \left| \frac{1}{1 + \alpha V_0 I_0 \gamma_0} \right|^2, \tag{26}$$

where $4k_B(T_0/R_0)$ is the high-frequency limit which coincides with the PSD of the current fluctuation i_e that appears in Equation (1).

2.3. Electrothermal Model of Two Thermally Coupled Wires. The elements of the model used for the pair of thermally coupled wires are illustrated in Figure 4.

The thermal and electrical quantities (V, I, R, T, and θ) are duplicated and an additional coupling thermal conductance θ_{12} is present. In this study, we assume that the system is symmetrical (the two wires are symmetrical) and are biased

in such a way that they reach a symmetrical OP, which is defined by the following values for the quantities of interest:

$$\begin{aligned} V_1 &= V_2 = V_0, \\ I_1 &= I_2 = I_0, \\ T_1 &= T_2 = T_0, \\ R_1 &= R_2 = R_0, \\ \theta_1 &= \theta_2 = \theta_0. \end{aligned} \tag{27}$$

In the majority of applications, thermally coupled wires are biased with a symmetrical operating point. On the other hand, variations are different between the two wires, so that the total values (OP plus variations) of the key quantities will be different from one wire to the other.

Equation (4), pertinent to a single wire, is replaced by the following set:

$$\begin{cases} C_{\mathrm{TH}} \dfrac{dT_1}{dt} = W_1 - \theta_1(T_1 - T_A) - \theta_{12}(T_1 - T_2), \\ C_{\mathrm{TH}} \dfrac{dT_2}{dt} = W_2 - \theta_2(T_2 - T_A) + \theta_{12}(T_1 - T_2). \end{cases} \tag{28}$$

In Equation (28), a heat exchange term due to conductance θ_{12} is clearly present. In terms of variations and Laplace transforms, we obtain

$$\begin{cases} sC_{\mathrm{TH}}\delta T_1 = w_1 - [\theta_0 + \beta\theta_0(T_0 - T_A)]\delta T_1 - \theta_{12}(\delta T_1 - \delta T_2), \\ sC_{\mathrm{TH}}\delta T_2 = w_2 - [\theta_0 + \beta\theta_0(T_0 - T_A)]\delta T_2 + \theta_{12}(\delta T_1 - \delta T_2). \end{cases} \tag{29}$$

Heat generation in the wires is described by the following set:

$$\begin{cases} w_1 = v_1 I_0 + i_1 V_0, \\ w_2 = v_2 I_0 + i_2 V_0, \end{cases} \tag{30}$$

while Equation (14) (Ohm's law plus Jonson-Nyquist current fluctuations) for the two wires is replaced by the following set:

$$\begin{cases} I_1 = \dfrac{V_1}{R_1} - i_{e1}, \\ I_2 = \dfrac{V_2}{R_2} - i_{e2}, \end{cases} \Longleftrightarrow \begin{cases} V_1 = I_1 R_1 + R_1 i_{e1}, \\ V_2 = I_2 R_2 + R_2 i_{e2}, \end{cases} \tag{31}$$

which, in terms of variations, becomes

$$\begin{cases} v_1 = i_1 R_0 + \alpha R_0 I_0 \delta T_1 + I_0 \delta R_{e1} + R_0 i_{e1}, \\ v_2 = i_2 R_0 + \alpha R_0 I_0 \delta T_2 + I_0 \delta R_{e2} + R_0 i_{e2}. \end{cases} \tag{32}$$

At this point, it is convenient to separate all variations into a differential mode and common mode component. For example, we will replace v_1 and v_2 by $v_{\mathrm{d}} = v_1 - v_2$ and $v_{\mathrm{c}} = (v_1 + v_2)/2$, respectively, where v_{d} is the differential component and v_{c} the common mode one. In the remainder of this document, differential mode and common mode quantities will be indicated with the "d" and "c" subscript, respectively. In this way, we can easily find decoupled equations for the differential mode and common mode variables. For the common mode components, the resulting equations are identical to those of the single wire. This is reasonable, since common mode components do not break the symmetry, and with no temperature difference, the two wires do not interact and behave as a single wire. Equations for the differential components are only slightly different, due to the presence of θ_{12}, so that from the Equation set (29), we can derive the following differential mode equation:

$$sC_{\mathrm{TH}}\delta T_{\mathrm{d}} = w_{\mathrm{d}} - [\theta_0 + \beta\theta_0(T_0 - T_A)]\delta T_{\mathrm{d}} - 2\theta_{12}\delta T_{\mathrm{d}}, \tag{33}$$

while from the Equation sets (30) and (32), we find differential mode equations that are identical to Equations (14) and (15), respectively:

$$\begin{cases} v_{\mathrm{d}} = i_{\mathrm{d}} R_0 + \alpha R_0 I_0 \delta T_{\mathrm{d}} + I_0 \delta R_{\mathrm{ed}} + R_0 i_{\mathrm{ed}}, \\ w_{\mathrm{d}} = v_{\mathrm{d}} I_0 + i_{\mathrm{d}} V_0. \end{cases} \tag{34}$$

From Equation (33), we can find the expression of δT_{d}, analogous to Equation (10):

$$\delta T_{\mathrm{d}} = \gamma_{\mathrm{d}}(s) w_{\mathrm{d}}, \tag{35}$$

$$\gamma_{\mathrm{d}}(s) = \frac{\gamma_{0\mathrm{d}}}{1 + s/\omega_{g\mathrm{d}}}, \tag{36}$$

$$\gamma_{0\mathrm{d}} = \frac{1}{\theta_0[1 + \beta(T_0 - T_A)] + 2\theta_{12}}, \tag{37}$$

$$\omega_{g\mathrm{d}} = \frac{1}{C_{\mathrm{TH}}\gamma_{0\mathrm{d}}}. \tag{38}$$

Since Equations (34)–(38) are formally equivalent to the equations of the single wire, with the sole difference of the expression of $\gamma_{0\mathrm{d}}$ (that replaces γ_0), the solution has the same form as Equation (17):

$$v_{\mathrm{d}} = i_{\mathrm{d}} \cdot r_{\mathrm{d}} + i_{\mathrm{ed}} \cdot r_{\mathrm{ed}} + k_{R\mathrm{d}} \delta R_{\mathrm{ed}}, \tag{39}$$

where

$$\begin{cases} r_{\mathrm{d}} = R_0 \dfrac{1 + \alpha V_0 I_0 \gamma_{0\mathrm{d}}}{1 - \alpha V_0 I_0 \gamma_{0\mathrm{d}}} \cdot \dfrac{1 + s/\omega_{z\mathrm{d}}}{1 + s/\omega_{p\mathrm{d}}}, \\ r_{\mathrm{ed}} = R_0 \dfrac{1}{1 - \alpha V_0 I_0 \gamma_{0\mathrm{d}}} \cdot \dfrac{1 + s/\omega_{g\mathrm{d}}}{1 + s/\omega_{p\mathrm{d}}}, \\ k_{Rd} = \dfrac{I_0}{1 - \alpha V_0 I_0 \gamma_{0\mathrm{d}}} \cdot \dfrac{1 + s/\omega_{g\mathrm{d}}}{1 + s/\omega_{p\mathrm{d}}}, \end{cases} \tag{40}$$

$$\omega_{z\mathrm{d}} = \omega_{g\mathrm{d}}(1 + \alpha W_0 \gamma_{0\mathrm{d}}),$$

$$\omega_{p\mathrm{d}} = \omega_{g\mathrm{d}}(1 - \alpha W_0 \gamma_{0\mathrm{d}}).$$

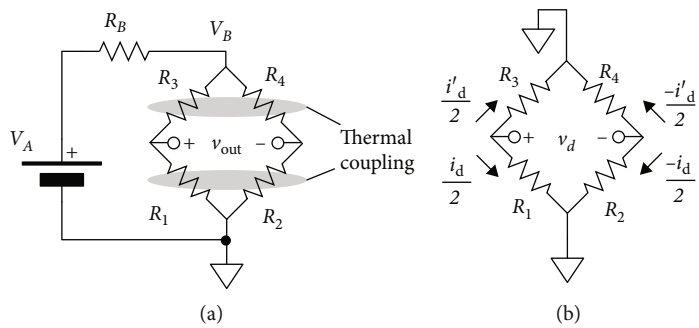

Figure 5: (a) Wheatstone bridge formed by two thermally coupled wire pairs; (b) equivalent circuit for differential mode variations.

In order to explain the way to use Equation (39) in a practical case, we can consider the very common situation in which the wires are biased with identical constant currents and the output signal is the voltage difference $v_d = v_1 - v_2$. In the next subsection, we will analyse the more complex case of a full Wheatstone bridge. With constant-current bias, both i_1 and i_2 are forced to be zero and then also i_d is zero. The forcing terms, i.e., Jonson-Nyquist current fluctuations i_{e1} and i_{e2} and resistance fluctuations δR_{e1} and δR_{e2}, are split into their common mode and differential mode components. Thanks to linearity of the small-signal equations and the fact that the equations are decoupled, we can calculate the effects of the two modes separately and then add them up. Common mode forcing terms produce only common mode variations, thus the effect on $v_{out} = v_d$ is null. Therefore, we can focus only on the differential mode terms. From Equation (39) with $i_d = 0$ and considering that i_{e1}, i_{e2}, δR_{e1}, and δR_{e2} are independent stochastic processes, we can find the PSD of the output voltage:

$$S_{vd}(f) = 2S_{ie}(f)|r_{ed}|^2 + 2S_{\delta Re}|k_{Rd}|^2, \tag{41}$$

where $S_{ie}(f) = 4k_B(T_0/R_0)$ and $S_{\delta Re}(f)$ are the PSD of the Johnson-Nyquist (thermal) current fluctuations and resistance fluctuations, respectively, of each single wire. Again, as in the case of the single wire, a boosting effect of both thermal and flicker noise at low frequencies is predicted if the TCR is positive. For the same heating power ($V_0 I_0$) and then the same overheating, we can expect a smaller noise increase with respect to the case of the single wire, due to the presence of the additional coupling term θ_{12} in γ_{0d}, compared to γ_0 of the single wire.

2.4. Noise in Wheatstone Bridges of Thermally Coupled Wire Pairs. Often, thermally coupled wire pairs are connected to form Wheatstone bridges as shown in Figure 5(a), where the two wire pairs are represented by resistors pairs R_1 and R_2 and R_3 and R_4. Since the aim is generally to sense a physical quantity, connection should be made in such a way that the effect of the quantity of interest contributes to the output voltage in a constructive way. The bridge can be biased with different approaches, which are all equivalent in terms of the effect of noise on the output voltage. In the example of Figure 5, the bridge is biased by a dc voltage source V_A (e.g., a battery) and a resistor R_B, which forms a voltage divider with the bridge resistance setting the operating voltage of the bridge to V_B.

The equivalent circuit for differential mode variations is represented in Figure 5(b), where the differential currents of the two wire pairs are indicated. Equation (39) for the two wire pairs becomes

$$\begin{cases} v_d = i_d \cdot r_d + i_{ed} \cdot r_{ed} + k_{Rd}\delta R_{ed}, \\ v_d{}' = i_d{}' \cdot r_d + i_{ed}{}' \cdot r_{ed} + k_{Rd}\delta R_{ed}{}', \end{cases} \tag{42}$$

where variables with a prime character $v_d{}'$, $i_d{}'$, $i_{ed}{}'$, and $\delta R_{ed}{}'$ belong to the upper wire pair of the bridge (R_3, R_4). By elementary analysis of the circuit in Figure 5(b), it is possible to find that $v_d{}' = v_d$ and $i_d{}' = -i_d$. Solving Equation set (42) with these relationships gives

$$2v_d = \left(i_{ed} - i_{ed}{}'\right) \cdot r_{ed} + k_{Rd}\left(\delta R_{ed} - \delta R_{ed}{}'\right). \tag{43}$$

Considering that i_{ed}, $i_{ed}{}'$, δR_{ed}, and $\delta R_{ed}{}'$ can be reasonably considered independent stochastic processes, and recalling the dependence of each one of these quantities with current fluctuations (i_e) and resistance fluctuations (δR_e) of the single wires of the bridge, we can finally find

$$S_{vd}(f) = S_{ie}(f)|r_{ed}|^2 + S_{\delta Re}|k_{Rd}|^2, \tag{44}$$

where, again, $S_{ie}(f) = 4k_B T/R_0$. Equation (44) indicates that the output noise PSD of a Wheatstone bridge is subjected to noise-boosting effects caused by overheating and that this effect is characterized by the differential mode parameters r_{ed} and k_{Rd}.

2.5. Determination of the Main Parameters. In order to utilize the proposed model to predict the output noise of single hot wires or arrangements of thermally coupled wires, it is necessary to find the system parameters. Referring to Equation set (18), it is possible to estimate all required parameters of a single wire by measuring the small-signal impedance (r) as a function of frequency. Fitting the response by means of a bilinear (one pole, one zero) function, it is possible to find ω_p and ω_z. From these two singularities, we can find ω_g and the $\alpha V_0 I_0 \gamma_0$ term. By these four quantities, it is possible to calculate coefficients r, r_e, and k_R as a function of

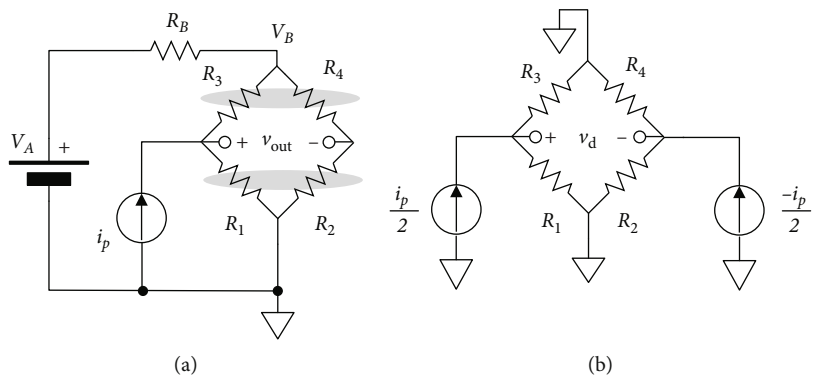

Figure 6: (a) Simulation of a Wheatstone bridge to calculate the differential mode parameters; (b) equivalent circuit for differential mode variations.

frequency (see Equation (18)). Measurements have to be performed by biasing the wire in the desired OP. To complete determination of the quantities present in Equation (17), it is also necessary to measure the spectrum of the resistance fluctuations ($S_{\delta Re}$) at different temperatures, by placing the wire in an oven to set the desired temperature without resorting to self-heating in order to avoid the mentioned noise-boosting effect.

The same parameters of a set of thermally coupled wires connected to form a Wheatstone bridge can be measured again from a single frequency sweep, using a current source i_p as in Figure 6(a).

Source i_p should have zero dc value and a sinusoidal ac component small enough to induce only a small displacement of the current and voltage of the bridge around the OP. Since we have demonstrated that only differential mode components contribute to the output PSD of the bridge, we can analyse only the differential mode equivalent circuit of Figure 6(b) where we can easily find that $i_d + i_d{}' = i_p$. Solving Equation set (42) with this condition and neglecting the noise components, we get

$$r_d = \frac{2v_d}{i_p}. \tag{45}$$

Sweeping the frequency of the source i_p and measuring voltage v_d, it is possible to use Equation (45) to calculate the frequency response of r_d from which the main parameters of the differential mode model can be determined.

3. Results and Discussion

In this section, we compare the predictions of our model with respect to those that can be obtained from the approach proposed in [15]. The comparison will be limited to the boosting factor of the thermal noise, since no effects of the electrothermal feedback on the flicker noise were proposed in the previous work.

Figure 7 shows the noise voltage PSD of the thermal noise, normalized with respect to the high-frequency limit. Note that this limit is the same for the two models and is

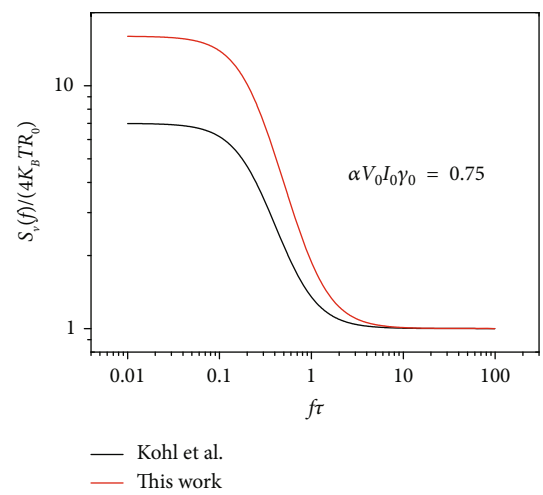

Figure 7: Calculated thermal noise PSD as a function of frequency, normalized to the high-frequency limit, for the proposed model and for the expression given in reference [15].

equal to $4k_BT_0R_0$, where R_0 is the wire resistance (V/I) ratio at the operating temperature. Both curves have been calculated for a value of parameter $\alpha V_0 I_0 \gamma_0$ equal to 0.75. We recall here that in [15], the noise density is simply assumed to be $4k_BT_0$ Re (r), while in the proposed model, the PSD is given by $4k_B(T_0/R_0)|r_e|^2$ (see the thermal component in Equation (23)). Figure 7 clearly shows that the two models predict a similar frequency behaviour but with noise boosting occurring at low frequencies which is significantly larger for the proposed model.

The dependence of the noise-boosting factor, $S_v(0)/S_v(\infty)$ on the parameter $\alpha V_0 I_0 \gamma_0$ is shown in Figure 8 for the two models. Negative values of $\alpha V_0 I_0 \gamma_0$ occur for negative values of the TCR. In both models, thermal noise is boosted at low frequencies for $\alpha > 0$ and reduced for $\alpha < 0$, but the extent of this effect is different in the two cases. The proposed model predicts more noise boosting for $\alpha > 0$ and less noise reduction for $\alpha < 0$ than the model in [15], for which the noise PSD tends to zero when $\alpha V_0 I_0 \gamma_0$ approaches -1.

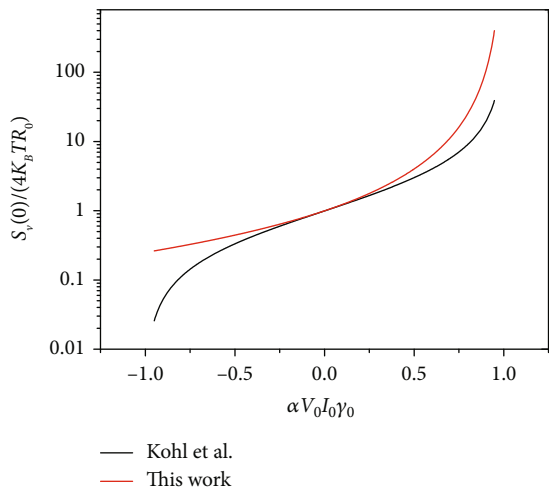

Figure 8: Ratio of the thermal noise PSD at 0 Hz (dc) over the high-frequency limit as a function of parameter $\alpha V_0 I_0 \gamma_0$, for the proposed model and for the model in reference [15].

Figures 7 and 8 demonstrate that the proposed model gives results that are significantly different from the previous model, and this enables discrimination between the two by means of noise measurements.

4. Conclusions

The analysis presented in this paper predicts in a quantitative way that the electrothermal feedback, resulting from the combination of self-heating with a nonzero TCR, changes the noise spectral density of a conducting wire. Both thermal noise and flicker noise are affected by a filtering effect that, depending on the sign of the TCR, boosts or dampens the noise density at low frequencies. This effect was already suggested in a previous work [15], where, however, an arbitrary assumption was made on the expression of the thermal noise PSD. The proposed model derives the thermal noise PSD with straightforward passages, starting from well-established properties of the thermal current fluctuations, and, in addition, is capable of predicting the effect also on the flicker noise spectrum. The approach is extended to pairs of thermally coupled wires, which constitute the core of thermal flow sensors and, more recently, have been proven capable of detecting acoustic particle velocity. In the proposed model, the filtering effect is characterized by parameters that can be easily determined by means of small-signal impedance measurements as a function of frequency.

Calculations of the thermal PSD performed using the proposed model and the previous approach revealed that the two models yield significantly different predictions of the noise modification occurring at low frequency. This should facilitate discriminating the two models through noise measurements, considering also that in both cases, the model parameters can be easily determined by means of small-signal impedance measurements as a function of frequency. These experiments should contribute to widen the knowledge of noise in out-of-equilibrium electrical systems.

Data Availability

The data used to support the findings of this study are included within the article.

Conflicts of Interest

The authors declare that there is no conflict of interest regarding the publication of this paper.

References

[1] J.-S. Shie, B. C. S. Chou, and Y.-M. Chen, "High performance Pirani vacuum gauge," *Journal of Vacuum Science & Technology A: Vacuum, Surfaces, and Films*, vol. 13, no. 6, pp. 2972–2979, 1995.

[2] P. Sturesson, L. Klintberg, and G. Thornell, "Pirani microgauge fabricated of high-temperature co-fired ceramics with integrated platinum wires," *Sensors and Actuators A: Physical*, vol. 285, pp. 8–16, 2019.

[3] J. Ruellan, J. Arcamone, D. Mercier, C. Dupré, and L. Duraffourg, "Pirani gauge based on alternative self-heating of silicon nanowire," in *2013 Transducers & Eurosensors XXVII: The 17th International Conference on Solid-State Sensors, Actuators and Microsystems (TRANSDUCERS & EUROSENSORS XXVII*, pp. 2568–2571, Barcelona, Spain, June 2013.

[4] A. Mahdavifar, M. Navaei, P. J. Hesketh, M. Findlay, J. R. Stetter, and G. W. Hunter, "Transient thermal response of micro-thermal conductivity detector (μTCD) for the identification of gas mixtures: an ultra-fast and low power method," *Microsystems & Nanoengineering*, vol. 1, no. 1, article 15025, 2015.

[5] A. Vatani, P. L. Woodfield, and D. V. Dao, "A miniaturized transient hot-wire device for measuring thermal conductivity of non-conductive fluids," *Microsystem Technologies*, vol. 22, no. 10, pp. 2463–2466, 2016.

[6] J. Chen and C. Liu, "Development and characterization of surface micromachined, out-of-plane hot-wire anemometer," *Journal of Microelectromechanical Systems*, vol. 12, no. 6, pp. 979–988, 2003.

[7] K. Kokmanian, S. Scharnowski, M. Bross et al., "Development of a nanoscale hot-wire probe for supersonic flow applications," *Experiments in Fluids*, vol. 60, no. 10, p. 150, 2019.

[8] B. Idjeri, M. Laghrouche, and J. Boussey, "Wind measurement based on MEMS micro-anemometer with high accuracy using ANN technique," *IEEE Sensors Journal*, vol. 17, no. 13, pp. 4181–4188, 2017.

[9] H.-E. de Bree, H. V. Jansen, T. S. J. Lammerink, G. J. M. Krijnen, and M. Elwenspoek, "Bi-directional fast flow sensor with a large dynamic range," *Journal of Micromechanics and Microengineering*, vol. 9, no. 2, pp. 186–189, 1999.

[10] H.-E. de Bree, P. Leussink, T. Korthorst, H. Jansen, T. S. J. Lammerink, and M. Elwenspoek, "The μ-flown: a novel device for measuring acoustic flows," *Sensors and Actuators A: Physical*, vol. 54, no. 1-3, pp. 552–557, 1996.

[11] O. Pjetri, R. J. Wiegerink, and G. J. Krijnen, "A 2D particle velocity sensor with minimal flow-disturbance," *IEEE Sensors Journal*, vol. 16, pp. 8706–8714, 2016.

[12] M. Piotto, F. Butti, E. Zanetti, A. Di Pancrazio, G. Iannaccone, and P. Bruschi, "Characterization and modeling of CMOS-compatible acoustical particle velocity sensors for applications

requiring low supply voltages," *Sensors and Actuators A: Physical*, vol. 229, pp. 192–202, 2015.

[13] M. Piotto, A. Ria, D. Stanzial, and P. Bruschi, "Design and characterization of acoustic particle velocity sensors fabricated with a commercial post-CMOS MEMS process," in *2019 20th International Conference on Solid-State Sensors, Actuators and Microsystems & Eurosensors XXXIII (TRANSDUCERS & EUROSENSORS XXXIII*, pp. 1839–1842, Germany, June 2019.

[14] N. R. Krishnaprasad, M. Contino, S. P. Chepuri, D. F. Comesana, and G. Leus, "DOA estimation and beamforming using spatially under-sampled AVS arrays," in *2017 IEEE 7th International Workshop on Computational Advances in Multi-Sensor Adaptive Processing (CAMSAP)*, pp. 1–5, Netherlands Antilles, December 2017.

[15] F. Kohl, F. Keplinger, A. Jachimowicz, and J. Schalko, "A model of metal film resistance bolometers based on the electro-thermal feedback effect," *Sensors and Actuators A: Physical*, vol. 115, no. 2-3, pp. 308–317, 2004.

[16] H. Neff, A. M. N. Lima, G. S. Deep et al., "Nonlinearity and electrothermal feedback of high T_c transition edge bolometers," *Applied Physics Letters*, vol. 76, no. 5, pp. 640–642, 2000.

[17] H. Neff, I. A. Khrebtov, A. D. Tkachenko et al., "Noise, bolometric performance and aging of thin high T_c superconducting films on silicon membranes," *Thin Solid Films*, vol. 324, no. 1-2, pp. 230–238, 1998.

[18] A. Ambrozy, *Electronic Noise*, McGraw-Hill, New-York, 1982.

[19] A. J. Dekker, H. Hickman, and T. M. Chen, "A tutorial approach to the thermal noise in metals," *American Journal of Physics*, vol. 59, no. 7, pp. 609–614, 1991.

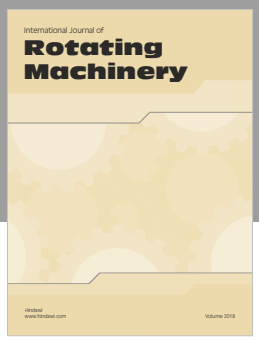

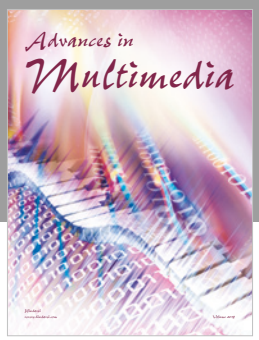

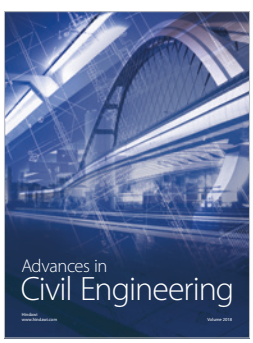

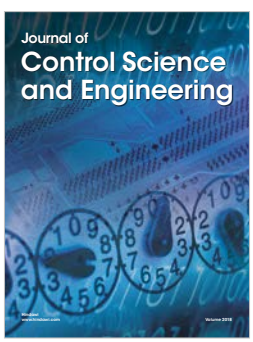

Hindawi
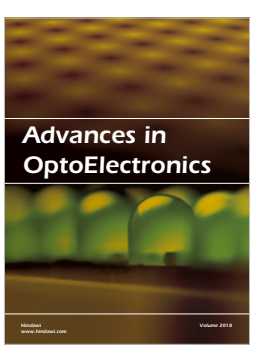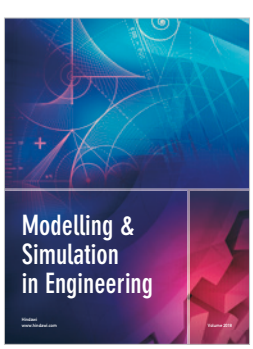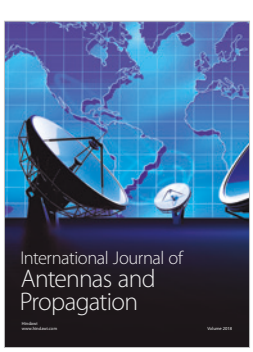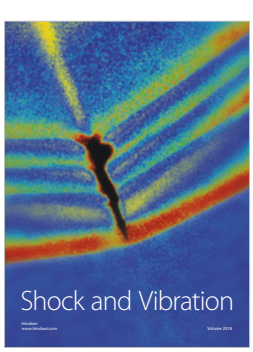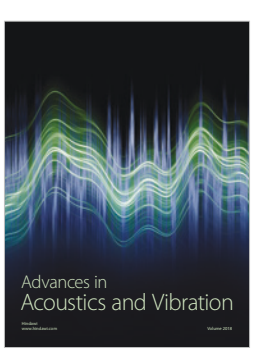
Submit your manuscripts at
www.hindawi.com